CDF note 9430

Search for High-Mass Resonances Decaying into Leptons of Different Flavor ($e\mu$, $\mu\tau$, $e\tau$)

The CDF Collaboration
URL http://www-cdf.fnal.gov
(Dated: September 16, 2009)

We present a search for a heavy sneutrino decaying to two leptons of different flavor, predicted in R-parity violating supersymmetric models. The search is based on 1 fb^{-1} of data collected in $p\bar{p}$ collisions by the CDF II Detector at the Fermilab Tevatron. Our results are consistent with the standard model expectations and we present upper limits on $\sigma \times \mathrm{BR}$ ($p\bar{p} \to \widetilde{\nu}_\tau \to e\mu, e\tau, \mu\tau$) calculated at 95% credibility level using a Bayesian approach.

I. INTRODUCTION

In the standard model (SM), conservation of baryon (B) and lepton (L) numbers is a consequence of the global symmetries in the theory. Even though B and L symmetries can be violated by non-perturbative effects [1], violation is small and doesn't lead to any contradictions with the experiment. The situation is quite different in the supersymmetric (SUSY) models where the gauge-invariant interactions involving superpartners of the SM particles (sparticles) can violate both B and L at tree-level and lead to proton decay times shorter than the current experimental limits [2]. In the minimal supersymmetric extension of the standard model (MSSM), these interactions can be described by the following superpotential terms:

$$\begin{aligned} W_{\Delta L=1} &= \frac{1}{2}\lambda^{ijk}\mathbf{L}_i\mathbf{L}_j\bar{\mathbf{e}}_k + \lambda^{'ijk}\mathbf{L}_i\mathbf{Q}_j\bar{\mathbf{d}}_k + \mu^{'i}\mathbf{L}_i\mathbf{H}_u, \\ W_{\Delta B=1} &= \frac{1}{2}\lambda^{''ijk}\bar{\mathbf{u}}_i\bar{\mathbf{d}}_j\bar{\mathbf{d}}_k \end{aligned} \quad (1)$$

where $\mathbf{L}$, $\mathbf{Q}$ and $\mathbf{H}$ are the $SU(2)$ doublet superfields of leptons, quarks and Higgs; $\bar{\mathbf{e}}$, $\bar{\mathbf{u}}$ and $\bar{\mathbf{d}}$ are the $SU(2)$ singlet superfields of leptons and quarks; λ, λ' and λ'' are Yukawa couplings; the indices i, j and k denote fermion generations and the terms in $W_{\Delta L=1}$ and $W_{\Delta B=1}$ violate L and B respectively. Proton decay could be avoided by postulating conservation of an additional quantum number, R-parity $P_R = (-1)^{3(B-L)+2s}$, where s is the particle spin [3]. Although each individual term in Eq.(1) corresponds to R-parity violating (RPV) interactions, proton decay requires simultaneous presence of both L- and B-violating terms. Therefore, RPV interactions conserving either B or L can produce rich physics beyond the SM, e.g., generate non-zero neutrino mass [4] and explain recently reported anomalous phase of the b to s transition [5], without contradicting the proton lifetime measurements [6]. A striking feature of models with RPV interactions is that in these models the lightest sparticle is no longer stable. Instead of escaping detection and producing events with large imbalance of momentum and energy it decays to the SM particles, completely changing experimental signatures of the SUSY processes. These models also allow processes of a single slepton production in hadron-hadron collisions. Slepton decays to a pair of SM leptons, reconstructed as resonances in the dilepton mass spectra, could signal presense of a new physics.

II. CDF II DETECTOR

The CDF II detector is a general purpose particle detector, described in detail elsewhere [10]. This measurement uses information from the central tracker [11], calorimeters [12, 13] and muon detectors [14] for charged lepton reconstruction and identification. Reconstruction of photons and π^0's makes extensive use of the CES, the central shower maximum detector which is embedded at a depth of six radiation lengths within the electromagnetic calorimeter [12]. The CES multiwire proportional chambers reconstruct position of the electromagnetic showers with an accuracy of $\sim$ 3 mm and have an energy resolution $\sigma(\mathrm{E})/\mathrm{E} \sim 30\%$. Luminosity is measured by a hodoscopic system of the Cherenkov counters [16].

The event geometry and kinematics are described using the azimuthal angle ϕ and the pseudorapidity $\eta = -\ln\tan\frac{\theta}{2}$, where θ is the polar angle with respect to the beamline. The transverse energy and momentum of the reconstructed particles and jets are defined in a standard way: $\mathrm{E_T} = \mathrm{E}\sin\theta$, $P_T = \mathrm{P}\sin\theta$, where E is the energy and P is the momentum.

III. TRIGGER AND DATA SAMPLES

The analysis is performed using 1 fb^{-1} of data collected in $p\bar{p}$ collisions at $\sqrt{s} = 1.96$ TeV by the CDF II detector at Fermilab.

The CDF data aquisition system is using a 3-level multipath trigger. The data used in the search were collected using inclusive high-P_T electron and muon triggers which select events with electrons and muon candidates with $P_T \geq$ 18 GeV and $|\eta| \lesssim 1.0$. In the region $P_T >$ 130 GeV the 18 GeV inclusive electron trigger starts loosing efficiency due to an inefficiency of the L2 electron selection. To compensate for that the analysis also includes events selected using an electron trigger with P_T threshold of 70 GeV which L2 part is 100% efficient in the high energy region.

IV. LEPTON RECONSTRUCTION AND IDENTIFICATION

Offline identification of the electron and muon candidates relies on the standard identification procedures described in [17], the lepton P_T threshold is raised to 20 GeV. Additional measurement of the electron energy in the CES helps to identify electron candidates that radiate significant fraction of their energy because of the bremsstrahlung and improves efficiency of the electron selection.

The τ leptons are identified via their hadronic decays as narrow calorimeter clusters pointed to by one or three charged tracks. As neutrino from the τ decay escapes detection, the "visible" four-momentum of a τ candidate, $\mathrm{P}_\tau^{\mathrm{vis}}$, is reconstructed as a sum of four-momenta of tracks and neutral particles pointing to a calorimeter cluster. Neutral particles are reconstructed using the CES showers that have no charged tracks pointing to them. We improve the resolution in $\mathrm{P}_\tau^{\mathrm{vis}}$ by combining measurements of the track momenta and energies of the CES showers with the energy measurements in the calorimeter. A τ candidate is required to have $\mathrm{E_T^{vis}} \geq 25\ GeV$ and its most energetic track must have $P_T > 10$ GeV/c. The reconstructed mass of a τ candidate, $\mathrm{M}_\tau^{\mathrm{vis}} = \sqrt{P_\tau^{vis\,2}}$, is required to be consistent with the τ lepton mass: $\mathrm{M}_\tau^{\mathrm{vis}} < 1.8 + 0.0455(\mathrm{E_T^{vis}} - 20)$, where the second term accounts for a degradation of the resolution in $\mathrm{M}_\tau^{\mathrm{vis}}$ at high energy. Reconstructed τ candidates consistent with an electron or a muon hypothesis are excluded from the analysis.

V. EVENT SELECTION

Events selected for analysis are required to have two identified central ($|\eta| < 1$) lepton candidates of different flavor and opposite electric charge. The leptons have to be isolated: the calorimeter energy measured within a cone of radius $\Delta\mathrm{R} \leq 0.4$ surrounding the leptons, where $\Delta\mathrm{R} = \sqrt{\Delta\eta^2 + \Delta\phi^2}$, must be less than 10% of the lepton energy. Events with leptons consistent with a photon conversion or a cosmic ray hypothesis are removed from the analysis sample.

VI. STANDARD MODEL BACKGROUNDS

We classify the backgrounds to this search based on the number of fake, resulting from misidentification, leptons in the event. The dominant source of the irreducible background are events with two real leptons in the final state produced in the processes of Drell-Yan ($Z/\gamma^* \rightarrow \tau\tau$), diboson ($WW$, WZ, ZZ) and top quark pair ($t\bar{t}$) production. A second class of the background events includes events with one fake lepton. These events come from the W+jet(s), Drell-Yan+jet(s) production with one of the jets misidentified as a lepton, and from Drell-Yan ($Z/\gamma^* \rightarrow ee$, $Z/\gamma^* \rightarrow \mu\mu$) production, where one of leptons is misidentified as a lepton of a different flavor. The backgrounds above are estimated using MC with the expectations normalized to the NLO cross sections [22–24].

The last class includes the background processes that produce events with two fake leptons. It is dominated by the QCD events with two jets misidentified as leptons and γ+jets events with a photon misidentified as an electron and a jet misidentified as a lepton (μ, τ). Their contribution is estimated from a data sample with two leptons of the same charge where we assume no charge correlation between the two misidentified leptons. To avoid double counting, same charge contribution of the background processes accounted for by the MC, is subtracted.

VII. CONTROL REGIONS

We use region 50 GeV/c^2 < M_{ll} < 110 GeV/c^2 as a control one to validate the event selection and the background normalization procedures.

The observed and expected event yields in the control region are in good agreement, as summarized in Table I. Good understanding of the sample composition in the control region is illustrated by Figure 1 which compares expected and observed distributions in $\mathrm{M}_\tau^{\mathrm{vis}}$ for $e\tau$ channel.

VIII. SIGNAL ACCEPTANCE

To calculate acceptance for the $\widetilde{\nu}_\tau$ production and its subsequent decay to a lepton pair we use the PYTHIA event generator with the modified decay table. We use NLO calculation of the $\widetilde{\nu}_\tau$ production cross section [21] to calculate the expected yield of the signal events.

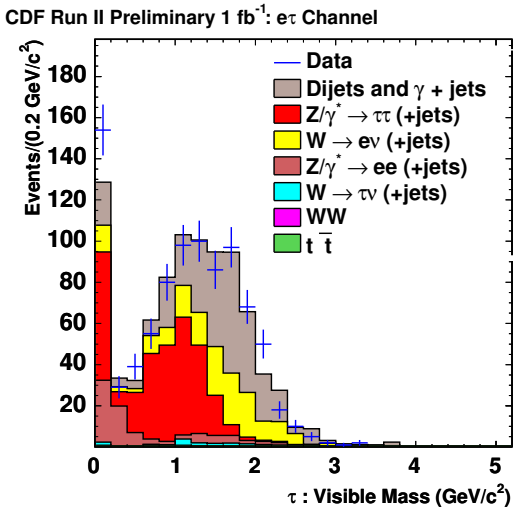

FIG. 1: Tau visible mass in the eτ channel control region.

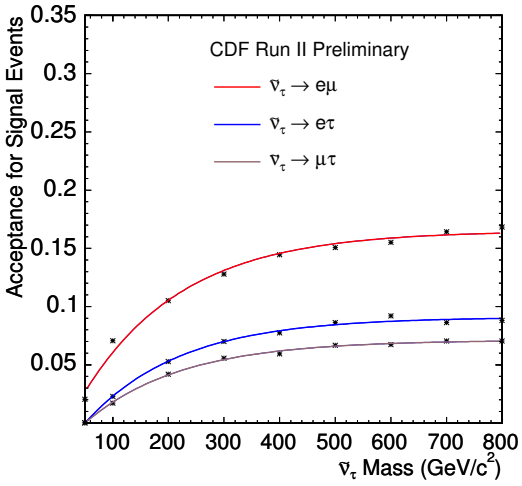

FIG. 2: The acceptance of $\widetilde{\nu}_\tau \to e\mu, e\tau, \mu\tau$. The acceptances for e$\tau$ and $\mu\tau$ channels are lower than for eμ channel because we only select hadronic τ and the τ ID efficiency is lower than electron and muon.

We take into account that $\widetilde{\nu}_\tau$ could be produced only in the process of $d\bar{d}$ annihilation not $u\bar{u}$ to guarantee the conservation of hypercharge.

The acceptance is calculated in 9 different mass points ranging from 50 GeV/c^2 to 800 GeV/c^2. The results are used to parameterize acceptance dependence on $M_{\widetilde{\nu}_\tau}$.

Full acceptance (geometrical acceptance convoluted with the trigger, reconstruction and identification efficiency) for all $e\mu$, $e\tau$ and $\mu\tau$ channels is shown in Figure 2 as a function of $\widetilde{\nu}_\tau$ mass, $M_{\widetilde{\nu}_\tau}$.

IX. SYSTEMATIC UNCERTAINTIES

The dominant systematic uncertainties in this search come from a number of sources. The relative uncertainty on the luminosity measurement is 6% [26]. Uncertainties on lepton identification efficiency are 3% for τ's, 1% for electrons and 1% for muons. The jet-to-τ misidentification probability is known to an accuracy of 15%. Uncertainties in the parton momentum distributions result in variations of the predicted signal cross section at a level of 4-20%,

depending on the $M_{\widetilde{\nu}_\tau}$, variations of the signal acceptance due to the same source are, however, less than 1%.

X. RESULTS

We calculate the expected and observed Bayesian limits on $\sigma(p\bar{p} \to \widetilde{\nu}_\tau) \times \mathrm{BR}(\widetilde{\nu}_\tau \to \mathrm{ll})$ at 95% credibility level (CL) as a function of $M_{\widetilde{\nu}_\tau}$ for different channels The calculation is performed using technique detailed in [25].

For a given value of $M_{\widetilde{\nu}_\tau}$, the limit is calculated by integrating the differential cross section $d\sigma/dM_{ll}$ over the region $M_{ll} > {M_{ll}}^{min}$, where the lower integration bound, ${M_{ll}}^{min}$, is chosen to optimize the search sensitivity for this $\widetilde{\nu}_\tau$ mass.

The optimization results depend on a signal-to-background ratio in a particular channel. For example, for $M_{\widetilde{\nu}_\tau} =$ 500 GeV/c^2, the optimized values of ${M_{ll}}^{min}$ are ${M_{ll}}^{min} = 310\mathrm{GeV}/c^2$ in $e\tau$ channel and ${M_{ll}}^{min} = 300\mathrm{GeV}/c^2$ in $\mu\tau$ channel.

In $e\mu$ channel, where the background is lower and the experimental resolution in $M_{\widetilde{\nu}_\tau}$ is better, the corresponding value of ${M_{ll}}^{min}$ is closer to the value of $M_{\widetilde{\nu}_\tau}$. For example, for $M_{\widetilde{\nu}_\tau} = 600$ GeV/c^2 the optimized position of the lower integration limit is ${M_{ll}}^{min} = 480$ GeV/c^2.

Table I shows the expected signal for $M_{\widetilde{\nu}_\tau} = 500$ GeV/c^2 and SM background in $e\tau$ and $\mu\tau$ channels and also the expected signal for $M_{\widetilde{\nu}_\tau} = 600$ GeV/c^2 and SM background in $e\mu$ channel. The observed event yields in data are consistend with the sum of expected contributions from the SM processes. As illustrated in Figure 3, we find no evidence of physics beyond the SM and set the 95% CL upper limits on the $\sigma \times$ BR of $\widetilde{\nu}_\tau$ as a function of a $\widetilde{\nu}_\tau$ mass. The expected and observed limits are shown in Figure 4 and in Table II. For a chosen set of RPV couplings the cross section limits can be converted into the limits on $M_{\widetilde{\nu}_\tau}$. Using values of $\lambda'_{311} = 0.10$, $\lambda_{132} = 0.05$, $\lambda_{133} = 0.05$ as a benchmark point, we obtain the following 95% CL limits on the $M_{\widetilde{\nu}_\tau}$: 482 GeV/c^2 in the $e\tau$ channel, 475 GeV/c^2 in the $\mu\tau$ channel and 556 GeV/c^2 in $e\mu$ channel.

XI. CONCLUSIONS

Using 1 fb^{-1} of data we have searched for a production of a heavy $\widetilde{\nu}_\tau$, decaying via RPV interactions to two leptons of different flavor: $e\mu$, $e\tau$ or $\mu\tau$. We find the data consistent with the SM predictions and set the 95% CL Bayesian limits on the $\sigma \times$ BR of $\widetilde{\nu}_\tau$ production. For a chosen set of RPV couplings ($\lambda'_{311} = 0.10$, $\lambda_{132} = 0.05$, $\lambda_{133} = 0.05$, $\lambda_{231} = 0.05$), the corresponding 95% CL limits on the $\widetilde{\nu}_\tau$ mass are 482 GeV/c^2 in the $e\tau$ channel, 475 GeV/c^2 in the $\mu\tau$ channel and 556 GeV/c^2 in the $e\mu$ channel.

[1] G.'t Hooft, Phys. Rev. Lett. **37**, 8 (1976).
[2] H. S. Goh, R.N. Mohapatra, S. Nasri, Siew-Phang Ng, Phys.Lett.B **587**, 105 (2004).
[3] G.R.Farrar and P. Fayet, Phys. Lett. B, **76**, 575 (1978); S. Dimopoulos, H. Georgi,Nucl. Phys. B **193**, 150 (1981); N. Sakai, T. Yanagida, Nucl. Phys. B **197**, 83 (1982); S. Weinberg, Phys. Rev. D **26**, 287 (1982).
[4] M. A. Diaz, C. Mora, A. R. Zerwekh, Eur.Phys.J.C **44**, 277 (2005).
[5] A. Kundu, S. Nandi, Phys.Rev.D **78**, 015009 (2008).
[6] Particle Data Group, R.M.Barnett *et al.*, Phys. Rev. D **54**, 85 (1996).
[7] R. Barbier *et al.*, Phys. Rept. **420**, 1 (2005).
[8] A. Abulencia *et al.* (CDF Collaboration), Phys. Rev. Lett. **96**, 211802 (2006).
[9] V. M. Abazov *et al.* (D0 Collaboration), Phys. Rev. Lett. **100**, 241803 (2008).
[10] R.Blair *et al.* (CDF-II Collaboration), FERMILAB-Pub-96/390-E.
[11] T. Affolder *et al.*, Nucl. Instrum. Methods Phys. Res. A**526**, 249 (2004).
[12] L. Balka *et al.*, Nucl. Instrum. Methods Phys. Res. A **267**, 272 (1988).
[13] S. Bertolucci, *et al.*, Nucl. Instrum. Methods Rhys. Res. A**267**, 301 (1988).
[14] G. Ascoli *et al.*, Nucl. Instrum. Methods Phys. Res. A**268**, 33 (1988).
[15] A.Byon-Wagner *et al.*, IEEE Trans. Nucl. Sci. **49**, 2567 (2002).
[16] D. Acosta *et al.*, Nucl.Instrum. Methods Phys. Res. A**494**, 57 (2002).
[17] A. Abulencia *et al.* (CDF Collaboration), J. Phys. G Nucl. Part. Phys. 34 (2007).
[18] T. Sjostrand *et al.*, Comput. Phys. Commun. **135**, 238 (2001).
[19] H. L. Lai *et al.*, Eur. Phys. J. C **12**, 375 (2000).

SM process	eτ channel
	M > 310GeV/c^2
$Z/\gamma^* \to \tau\tau$	0.2 ± 0.03
$Z/\gamma^* \to ee$	0.04 ± 0.01
$W \to e\nu$(+jets)	0.3 ± 0.05
$W \to \tau\nu$(+jets)	0.002 ± 0.001
WW	0.01 ± 0.002
$t\bar{t}$	0.004 ± 0.001
Dijets and γ +jets	0.3 ± 0.06
Total SM background	0.9 ± 0.06 ±0.1
Expected signal	2.7 ± 0.1 ±0.3
Observed Events in data	2

SM process	$e\mu$ channel
	M > 480GeV/c^2
$Z/\gamma^* \to \tau\tau$	0.002 ± 0.002
$Z/\gamma^* \to \mu\mu$	0.0005 ± 0.0003
$W \to \mu\nu$(+jets)	¡0.0001
WW	0.01± 0.001
$t\bar{t}$	0.002±0.002
Dijets and γ +jets	0.002±0.002
Total SM background	0.02±0.003±0.01
Expected signal	1.8 ± 0.05 ±0.2
Observed Events in data	0

SM process	$\mu\tau$ channel
	M > 300GeV/c^2
$Z/\gamma^* \to \tau\tau$	0.06 ± 0.02
$Z/\gamma^* \to \mu\mu$	0.07 ± 0.02
$W \to \mu\nu$(+jets)	0.25 ± 0.06
$W \to \tau\nu$(+jets)	0.002 ± 0.001
WW	0.02 ± 0.002
$t\bar{t}$	0.003 ± 0.002
Dijets	0.01 ± 0.003
Total SM background	0.4 ± 0.07 ± 0.1
Expected signal	2.0 ± 0.1 ± 0.2
Observed Events in data	0

TABLE I: The expected signal (M = 500GeV/c^2) and SM background in eτ and $\mu\tau$ channels. The expected signal (M = 600GeV/c^2) and SM background in eμ channel. The uncertainties on the individule background are statistic uncertainties. The uncertainties on the total SM background and expected signal are statistic and systematic uncertainties.

[20] R. Brun, R. Hagelberg, M. Hansroul, and J.C. Lassalle, CERN-DD-78-2-REV.
[21] S.-M. Wang et al., Phys. Rev. D **74**, 057902 (2006); Chinese Phys. Lett. **25**, 58 (2008).
[22] A.Abulencia et al (CDF collaboration), J. Phys. G Nucl. Part. Phys. **34**, 2457 (2007).
[23] J.M.Campbell and R.K Ellis, Phys.Rev. D **60**, 113006 (1999).
[24] N.Kidonakis, R.Vogt, Phys.Rev. **D78**, 074005 (2008).
[25] J.Heinrich and L.Lyons, Annual Review of Nuclear and Particle Science, **57**, 145 (2007).
[26] S. Klimenko, J. Konigsberg, and T.M. Liss, FERMILAB-FN-0741 (2003).

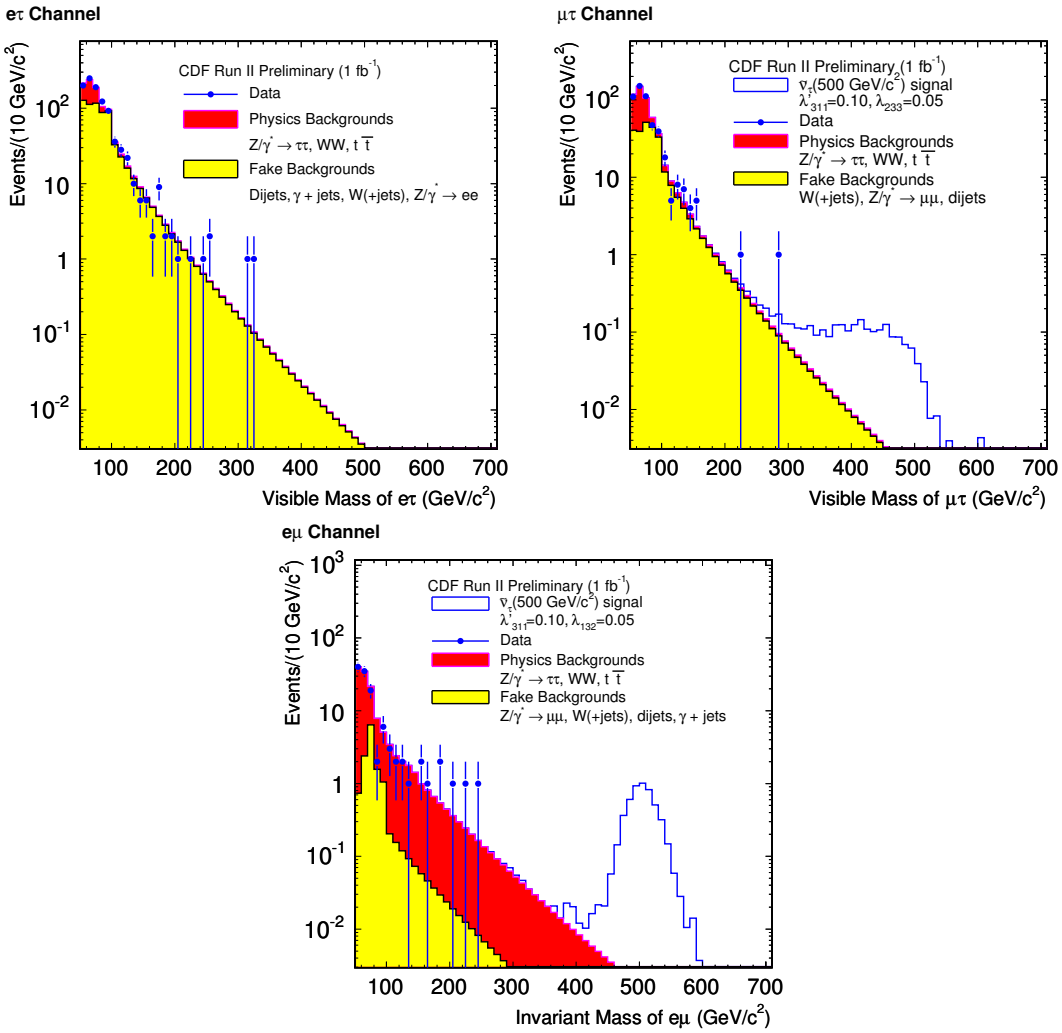

FIG. 3: The observed events in data agree with the expectation. We find no evidence of physics beyond SM.

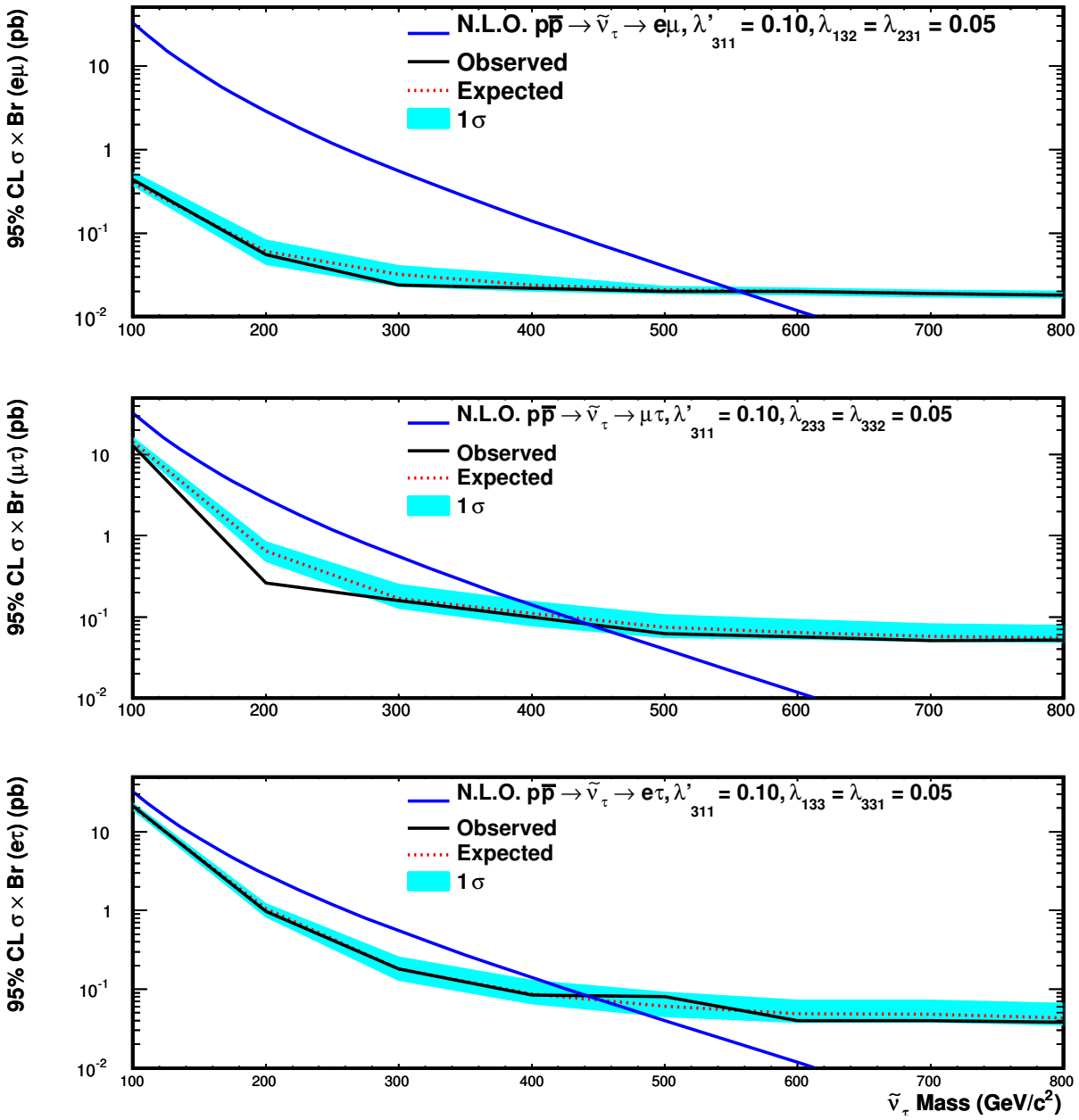

FIG. 4: The expected 95 % CL upper limits on the $\sigma \times$ BR $\widetilde{\nu}_\tau$ as a function of $\widetilde{\nu}_\tau$ mass. The observed 95 % CL upper limits on the $\sigma \times$ BR as a function of $\widetilde{\nu}_\tau$ mass shown as the black curve. For a chosen set of RPV couplings ($\lambda'_{311} = 0.10$, $\lambda_{132} = 0.05$, $\lambda_{133} = 0.05$, $\lambda_{233} = 0.05$), the limits on the $\widetilde{\nu}_\tau$ mass are 482 GeV/c^2 in the $e\tau$ channel, 475 GeV/c^2 in the $\mu\tau$ channel and 556 GeV/c^2 in $e\mu$ channel.

$e\tau$ channel						
signal mass (GeV/c^2)	mass cut (GeV/c^2)	SM background events	observed events	exp. signal events	exp. limit (pb)	obs. limit (pb)
100	> 80	335.9 ± 13.1	345	629.4 ± 45.7	20.88	21.28
200	> 160	22.7 ± 1.4	22	83.9 ± 4.9	1.05	0.97
300	> 230	5.0 ± 0.5	5	22.7 ± 1.1	0.18	0.18
400	> 280	2.1 ± 0.4	2	8.2 ± 0.3	0.087	0.084
500	> 310	1.4 ± 0.3	2	2.7 ± 0.1	0.061	0.081
600	> 340	1.0 ± 0.3	0	0.9 ± 0.03	0.049	0.040
700	> 360	0.9 ± 0.2	0	0.3 ± 0.01	0.048	0.040
800	> 360	0.9 ± 0.2	0	0.1 ± 0.003	0.043	0.038
$\mu\tau$ channel						
signal mass (GeV/c^2)	mass cut (GeV/c^2)	SM background events	observed events	exp. signal events	exp. limit (pb)	obs. limit (pb)
100	> 80	148.4 ± 9.9	135	417.2 ± 37.2	14.33	13.01
200	> 160	9.2 ± 1.2	2	62.9 ± 4.3	0.65	0.26
300	> 220	2.3 ± 0.3	1	17.2 ± 1.0	0.17	0.16
400	> 240	1.2 ± 0.2	0	5.8 ± 0.3	0.11	0.10
500	> 280	0.4 ± 0.1	0	2.0 ± 0.1	0.075	0.062
600	> 320	0.2 ± 0.04	0	0.63 ± 0.03	0.064	0.057
700	> 350	0.2 ± 0.04	0	0.21 ± 0.01	0.058	0.051
800	> 370	0.1 ± 0.02	0	0.06 ± 0.002	0.055	0.052
$e\mu$ channel						
signal mass (GeV/c^2)	mass cut (GeV/c^2)	SM background events	observed events	exp. signal events	exp.limit (pb)	obs.limit (pb)
100	> 90	23.0 ± 2.5	22	2305.5 ± 87.4	0.46	0.44
200	> 190	3.2 ± 0.3	3	292.7 ± 9.2	0.060	0.055
300	> 280	0.6 ± 0.1	0	70.0 ± 2.8	0.032	0.024
400	> 360	0.13 ± 0.02	0	19.7 ± 0.5	0.024	0.022
500	> 450	0.04 ± 0.01	0	5.9 ± 0.1	0.021	0.020
600	> 500	0.02 ± 0.03	0	1.8 ± 0.05	0.020	0.020
700	> 550	0.006 ± 0.001	0	0.6 ± 0.01	0.019	0.019
800	> 600	0.006 ± 0.001	0	0.2 ± 0.01	0.018	0.018

TABLE II: The observed limits on $\sigma \times$ BR of $\tilde{\nu}_\tau$. We quote the statistical uncertainty on SM background and expected signal. The expected and observed limits are calculated including the systematic uncertainties listed in the text.